5798 *Inorg. Chem.* **2010**, *49*, 5798–5810
DOI: 10.1021/ic100472p

Inorganic Chemistry
Award Article

Recent Applications of a Synthetic Model of Cytochrome *c* Oxidase: Beyond Functional Modeling†

James P. Collman* and Somdatta Ghosh‡

Department of Chemistry, Stanford University, Stanford, California 94305. ‡Present address: Department of Inorganic Chemistry, Indian Association for the Cultivation of Science, 2A & 2B Raja S. C. Mullick Road, Kolkata 700032, India.

Received March 11, 2010

This account reports recent developments of a functional model for the active site of cytochrome *c* oxidase (CcO). This CcO mimic not only performs the selective four-electron reduction of oxygen to water but also catalytically reduces oxygen using the biological one-electron reductant, cytochrome *c*. This functional model has been used to understand other biological reactions of CcO, for example, the interaction between the gaseous hormone, NO, and CcO. A mechanism for inactivating NO−CcO complexes is found to involve a reaction between oxygen and Cu_B. Moreover, NO is shown to be capable of protecting CcO from toxic inhibitors such as CN^- and CO. Finally, this functional CcO model has been used to show how H_2S could induce hibernation by reversibly inhibiting the oxygen binding step involved in respiration.

1. Introduction

Cytochrome *c* oxidase (CcO) is a multicomponent membrane-bound protein that catalyzes the four-electron reduction of oxygen (O_2) to water (H_2O) in all eukaryotes.[1−3] The energy released in this process is used to produce a proton gradient across the membrane, which provides the driving force for adenosine triphosphate (ATP) synthesis by ATPase.[4,5] The active site in CcO consists of a a bimetallic center comprising an iron porphyrin (heme a_3) and a tris-histidine-coordinated Cu (Cu_B) in the distal pocket.[2,3] There is also a post-translationally modified tyrosine residue covalently bound to one of the histidine residues ligated to the distal Cu_B (Figure 1A). During catalytic turnover, the reduced Fe^{II}/Cu^{I} center binds and reduces O_2, and the resulting oxidized site is reduced via rapid electron transfer from two additional electron-transfer sites present in CcO, heme a, and Cu_A, regenerating the reduced active site. These electrons are, in turn, derived from the cytochrome *c* (Cytc), which delivers them at a slower rate than the intra-electron-transfer rate.

Over the past several years, our laboratory has synthesized model complexes with the specific aim of structurally and functionally modeling the active site of CcO. Initial synthetic attempts using a pyridine/imidazole-based proximal tail and a macrocyclic ligand-based distal copper binding pocket have been discussed elsewhere.[6−14] Our most recent synthetic model has incorporated a myoglobin-like heme fitted with a covalently attached proximal imidazole and an array of three imidazoles coordinated to copper rigidly attached to the distal face of the iron porphyrin (Figure 1B). A phenol was appended to one distal imidazole.[15] These components

† This award article is an extended version of the Ronald Breslow Award for Achievement in Biomimetic Chemistry, 2009, presented at the 237th American Chemical Society National Meeting at Salt Lake City, UT.

*To whom correspondence should be addressed. E-mail jpc@stanford.edu.

(1) Ferguson-Miller, S.; Babcock, G. T. *Chem. Rev.* **1996**, *96*, 2889–2907.
(2) Iwata, S.; Ostermeier, C.; Ludwig, B.; Michel, H. *Nat. Rev. Drug Discovery* **1995**, *376*, 660–669.
(3) Yoshikawa, S.; Shinzawa-Itoh, K.; Nakashima, R.; Yaono, R.; Yamashita, E.; Inoue, N.; Yao, M.; Fei, M. J.; Libeu, C. P.; Mizushima, T.; Yamaguchi, H.; Tomizaki, T.; Tsukihara, T. *Science* **1998**, *280*, 1723–1729.
(4) Babcock, G. T.; Wikstrom, M. *Nat. Rev. Drug Discovery* **1992**, *356*, 301–309.
(5) Ludwig, B.; Bender, E.; Arnold, S.; Huttemann, M.; Lee, I.; Kadenbach, B. *ChemBioChem* **2001**, *2*, 392–403.
(6) Collman, J. P.; Herrmann, P. C.; Boitrel, B.; Zhang, X.; Eberspacher, T. A.; Fu, L.; Wang, J.; Rousseau, D. L.; Williams, E. R. *J. Am. Chem. Soc.* **1994**, *116*, 9783–9784.
(7) Collman, J. P.; Schwenninger, R.; Rapta, M.; Broring, M.; Fu, L. *Chem. Commun.* **1999**, *2*, 137–138.
(8) Collman, J. P.; Fu, L.; Herrmann, P. C.; Wang, Z.; Rapta, M.; Broring, M.; Schwenninger, R.; Boitrel, B. *Angew. Chem.* **1999**, *37*, 3397–3400.
(9) Collman, J. P.; Fu, L.; Herrmann, P. C.; Zhang, X. *Science* **1997**, *275*, 949–951.
(10) Collman, J. P. *Inorg. Chem.* **1997**, *36*, 5145–5155.
(11) Collman, J. P.; Broering, M.; Fu, L.; Rapta, M.; Schwenninger, R.; Straumanis, A. *J. Org. Chem.* **1998**, *63*, 8082–8083.
(12) Collman, J. P.; Zhong, M.; Wang, Z.; Rapta, M.; Rose, E. *Org. Lett.* **1999**, *1*, 2121–2124.
(13) Collman, J. P.; Rapta, M.; Broering, M.; Raptova, L.; Schwenninger, R.; Boitrel, B.; Fu, L.; L'Her, M. *J. Am. Chem. Soc.* **1999**, *121*, 1387–1388.
(14) Collman, J. P.; Boulatov, R.; Sunderland, C. J.; Fu, L. *Chem. Rev.* **2004**, *104*, 561–588.
(15) Collman, J. P.; Decreau, R. A.; Zhang, C. *J. Org. Chem.* **2004**, *69*, 3546–3549.

 Published on Web 06/07/2010

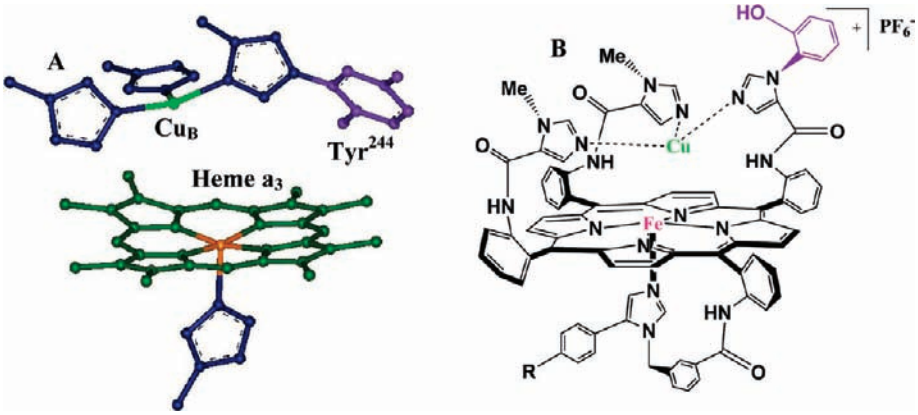

Figure 1. Active site structures of (A) CcO and (B) a synthetic model of CcO.

replicate the heme a_3, Cu_B, and Tyrosine^{244} residue, respectively. In this review, we focus on our most recent accomplishments using this newer family of ligands, discuss the strategy for synthesizing this model complex, and then demonstrate how this CcO mimic selectively catalyzes the four-electron reduction of O_2 at physiological pH and potential, under conditions of rate-limiting electron transfer. This catalyst also performs the stoichiometric four-electron reduction of O_2 using the actual biological reductant, Cytc as the source of electrons. Finally, the protective role of NO and the mechanism of H_2S inhibition of CcO using this functional synthetic model complex are presented.

James P. Collman was born in Beatrice, NE, in 1932 and received B.S. and M.S. degrees from the University of Nebraska in 1954 and 1956 and then a Ph.D. from the University of Illinois in 1958 under the supervision of R. C. Fuson. From 1958 to 1967, he was on the faculty of The University of North Carolina at Chapel Hill; in 1967, he moved to Stanford University, where he is Daubert Professor of Chemistry. His research interests are very broad, extending across inorganic and organic chemistry but also including superconductivity. His principal research is directed toward the invention and study of functional synthetic mimics of heme protein active sites. His work has been recognized by many awards, the most recent being the American Chemical Society Ronald Breslow Award for Achievement in Biomimetic Chemistry, 2009, and the American Academy of Arts and Sciences. He has been a member of the National Academy of Sciences since 1975.

2. Design and Synthesis

The synthetic strategies for the preparation of model complexes, developed in our group, over many years can be summarized into three categories: (i) face selection and insertion of the proximal imidazole ligand (Scheme 1), (ii) attachment of distal imidazole ligands (Scheme 2), and (iii) introduction of metals (Scheme 3).[16]

Face Selection and Insertion of the Proximal Imidazole Ligand. Nitrobenzaldehyde couples with pyrrole to generate a tetranitroporphyrin, which is subsequently reduced to form a mixture of four atropisomers of *meso*-tetrakis(*o*-aminophenyl)porphyrin.[17] This is derivatized by the addition of 1 equiv of trityl bromide.[11] The reaction mixture is heated and stirred over alumina, which causes slow isomerization until one isomer is selectively adsorbed on the alumina. This isomer contains three amine groups on one side of the porphyrin ring, with the bulky trityl group on the opposite side. The desired compound is washed away from alumina, and the three amine groups are then protected with trifluoroacetyl groups. In the following step, the trityl group is removed and an imidazole-substituted acid chloride introduced as the proximal imidazole ligand.[15,18,19] This imidazole-substituted acid chloride can be derivatized as required. A CF_3 group can be introduced for ^{19}F NMR studies, or a terminal alkyne group can be appended for clicking onto an azide-substituted self-assembled monolayer (SAM) film (discussed later).

Attachment of Distal Imidazole Ligands. As represented in Scheme 2, the next step involves deprotection of the three amine groups with ammonia, followed by introduction of two imidazole-substituted acid chlorides.[15,20] This leads to cis and trans regioisomers of the unsubstituted amine ligand. The desired cis isomer can be separated using a rotating chromatron.[20] The remaining free amine

(16) Collman, J. P.; Decreau, R. A. *Chem. Commun.* **2008**, *41*.
(17) Collman, J. P.; Gagne, R. R.; Reed, C.; Halbert, T. R.; Lang, G.; Robinson, W. T. *J. Am. Chem. Soc.* **1975**, *97*, 1427–1439.
(18) Collman, J. P.; Broering, M.; Fu, L.; Rapta, M.; Schwenninger, R. *J. Org. Chem.* **1998**, *63*, 8084–8085.
(19) Collman, J. P.; Sunderland, C. J.; Boulatov, R. *Inorg. Chem.* **2002**, *41*, 2282–2291.
(20) Decreau, R. A.; Collman, J. P.; Yang, Y.; Yan, Y.; Devaraj, N. K. *J. Org. Chem.* **2007**, *72*, 2794–2802.

Scheme 1. Face Selection and Insertion of the Proximal Imidazole Ligand

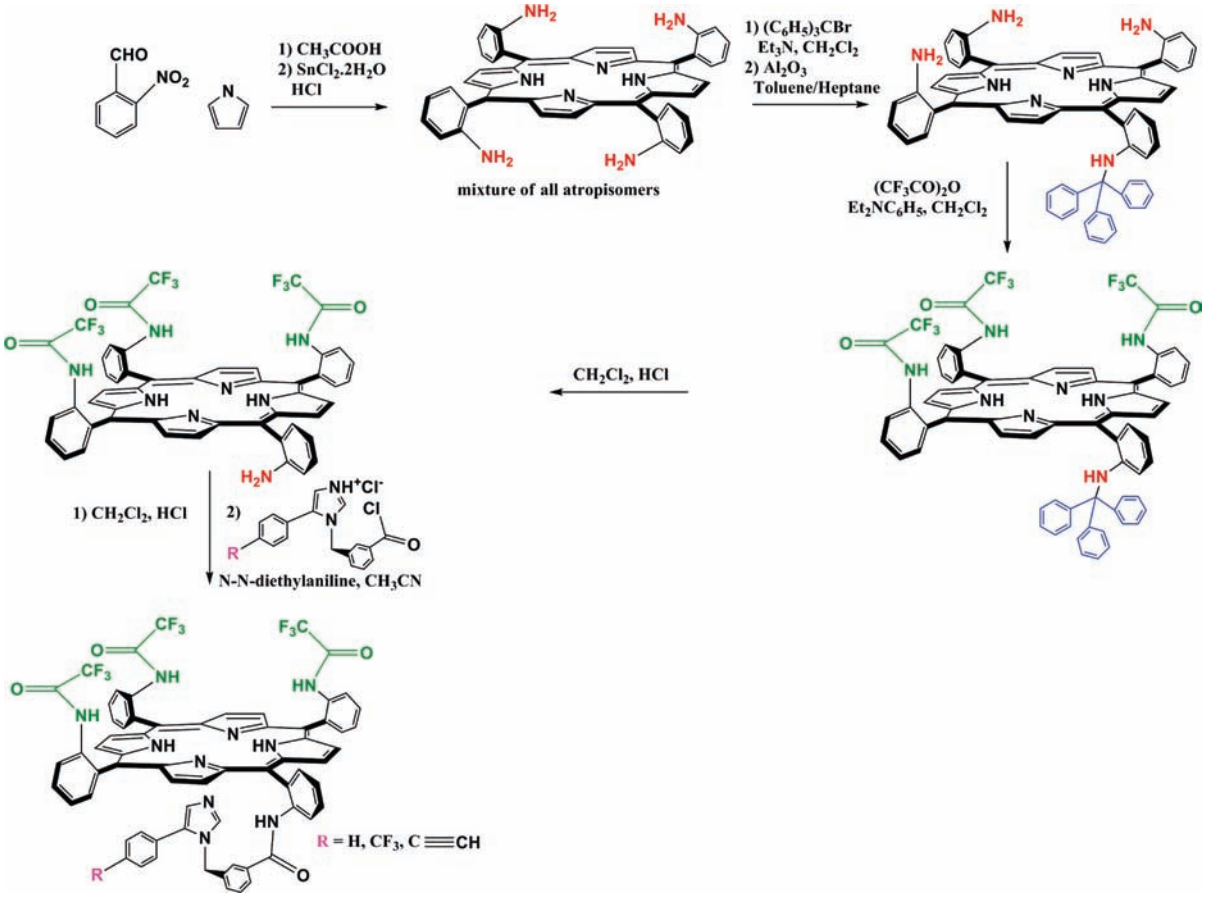

Scheme 2. Attachment of Distal Imidazole Ligands

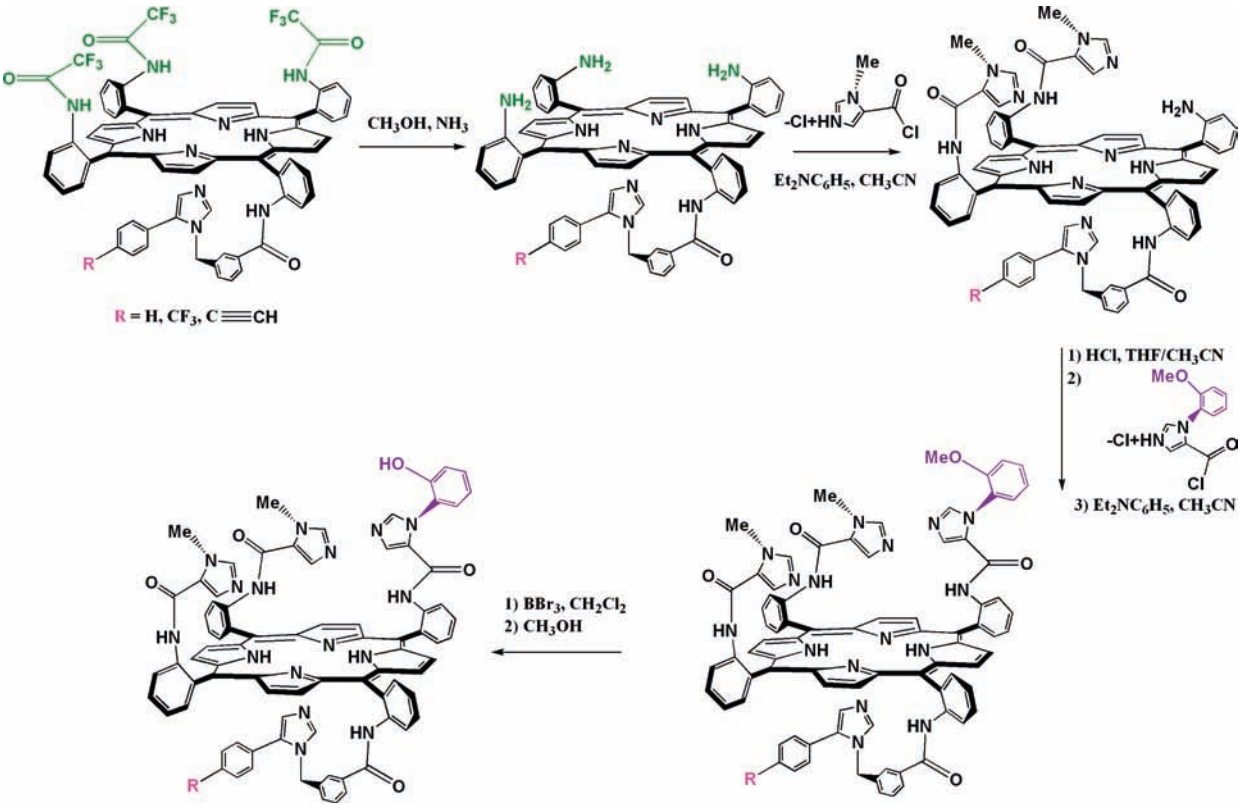

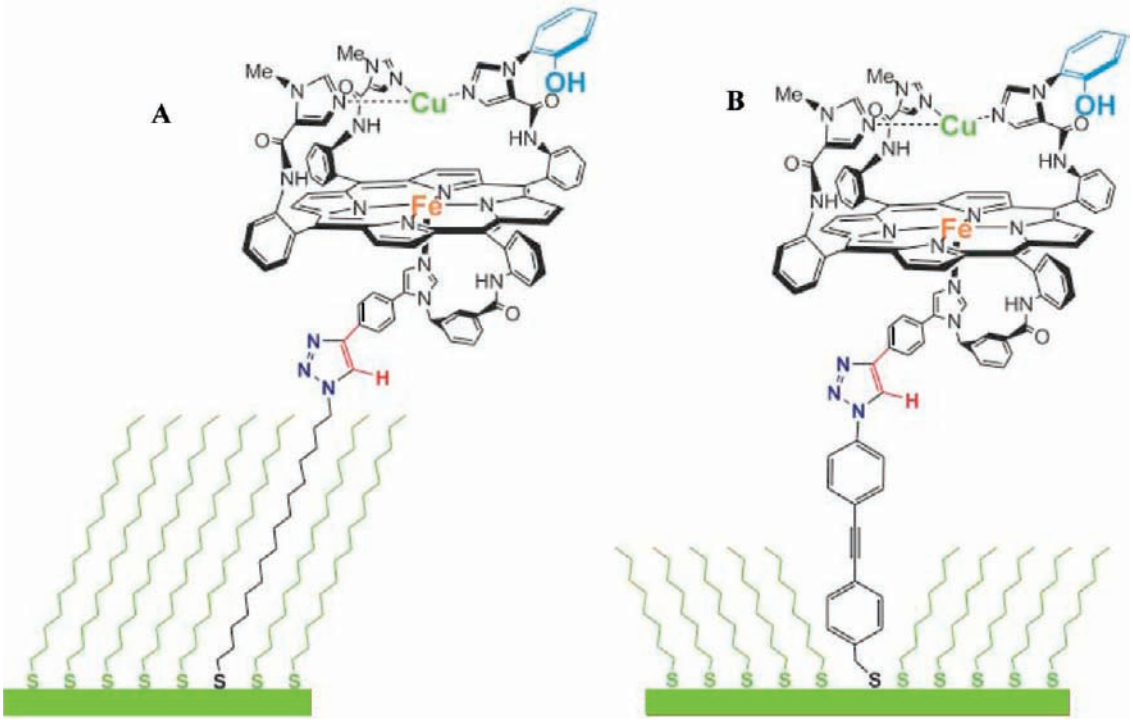

Figure 2. Catalyst clicked to (A) slow SAM and (B) fast SAM.

Scheme 3. Introduction of Metals

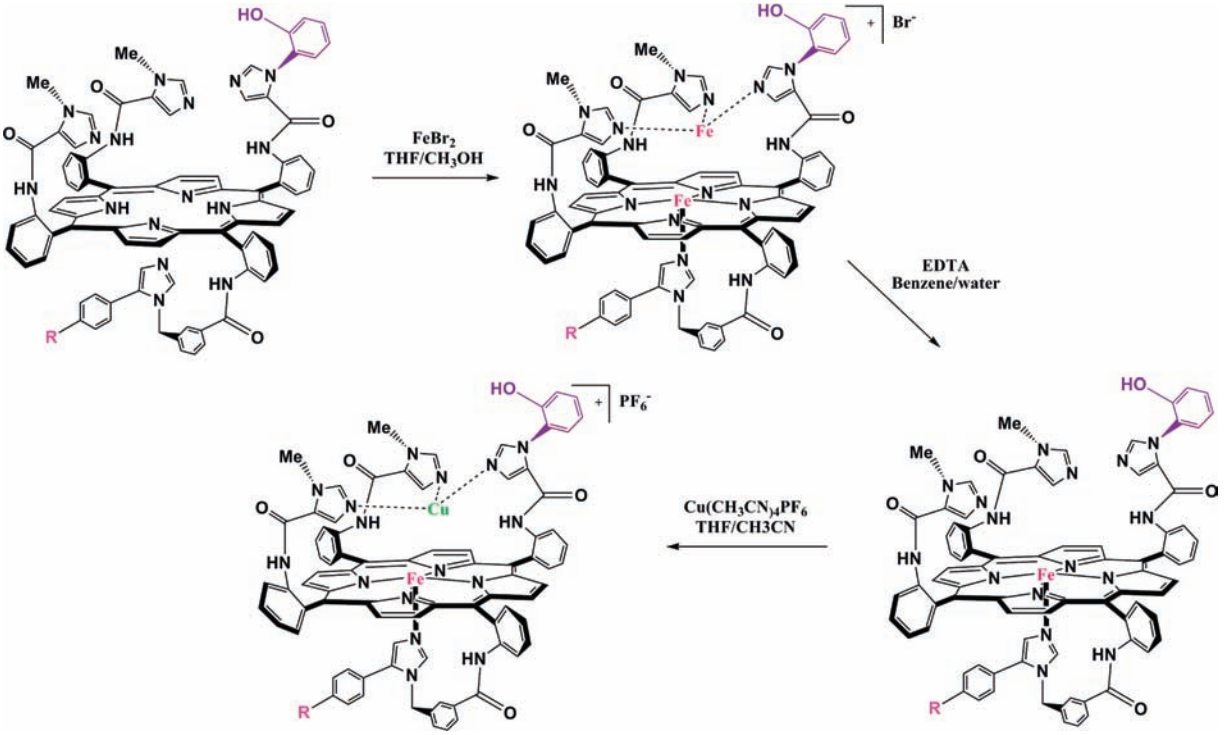

group is then derivatized using an imidazole-substituted acid chloride containing phenyl methyl ether. The methyl ether group is then deprotected using BBr_3, generating the phenol group.

Introduction of Metals. The remaining steps are illustrated in Scheme 3. Iron is introduced using a ferrous salt, which binds to both the porphyrin ring and the distal imidazole ligands.[19] An ethylenediaminetetraacetic acid wash selectively removes the distal iron. Then copper is introduced by adding a cuprous salt. This leads to the formation of the reduced $Fe^{II}Cu^{I}ArOH$ active catalyst.

3. Steady-State O_2 Reduction under Fast and Slow Electron Transfer

The four-electron reduction of O_2 to H_2O, without generating toxic, partially reduced oxygen species (PROS) is

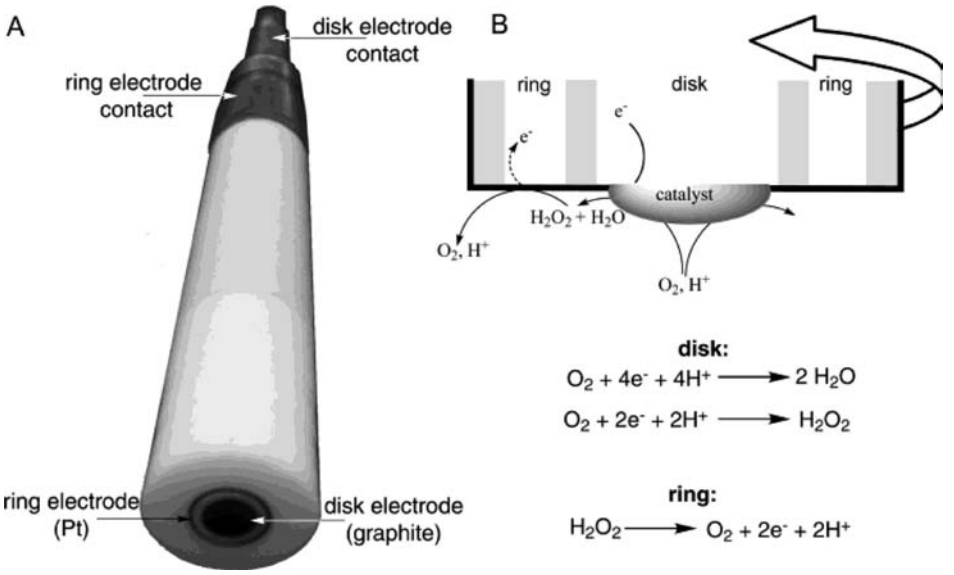

Figure 3. (A) Rotating-ring disk electrode (RRDE). (B) Schematic representation of the operation of the RRDE. Rotation of the electrode (block arrow) creates a flow of electrolytes containing the reactants (solid arrows) to the catalyst and sweeps the products of catalysis past the ring electrode. If the catalyst produces H_2O_2 (or superoxide), a portion of it is oxidized at the ring, producing a current (broken arrow).

highly challenging. In CcO, the steady-state rate of catalytic O_2 reduction is limited by the slow rate-determining electron transfer from Cytc (5−20 ms), which is the source of electrons for CcO. However, the rate of electron transfer within the CcO active site is about 10^3 times faster (20 μs).[16] The catalytic turnover in CcO occurs without the release of PROS. Our goal was to develop a functional model of CcO that can not only mimic the slow rate of electron delivery to the catalyst but also do so with minimal PROS production.

We developed a new method to carry out the electrocatalytic reduction of O_2. SAMs are prepared by chemisorption of desired-chain-length alkyl thiols on gold disk electrodes. The next step requires the coupling of the catalyst to the alkyl thiol. We utilize a Cu^I-catalyzed "click" reaction to couple the porphyrin catalyst to the SAM. An alkyne-terminated catalyst (R = terminal alkyne; Schemes 1−3) is coupled to azide-terminated alkyl thiols, resulting in quantitative and regiospecific 1,5 cycloaddition forming a stable triazole.[21]

Different chain lengths of the alkyl thiol were chosen to study the effect of both slow (Figure 2A) and fast electron transfer (Figure 2B) from the electrode to the catalyst.[22]

The rotating-ring disk technique can be used to measure the amount of PROS generated during the electrocatalytic reduction of O_2 (Figure 3). The disk electrode is maintained at a sufficiently negative potential (generally at −100 mV vs NHE) that causes the four-electron reduction of O_2 (determined from the Koutecky−Levich equation)[23] to H_2O and the two-electron reduction of O_2 to hydrogen peroxide (if any). The ring electrode is held at a constant, high potential (generally at +900 mV vs NHE) that oxidizes any hydrogen peroxide generated at the disk electrode to O_2. If the catalyst

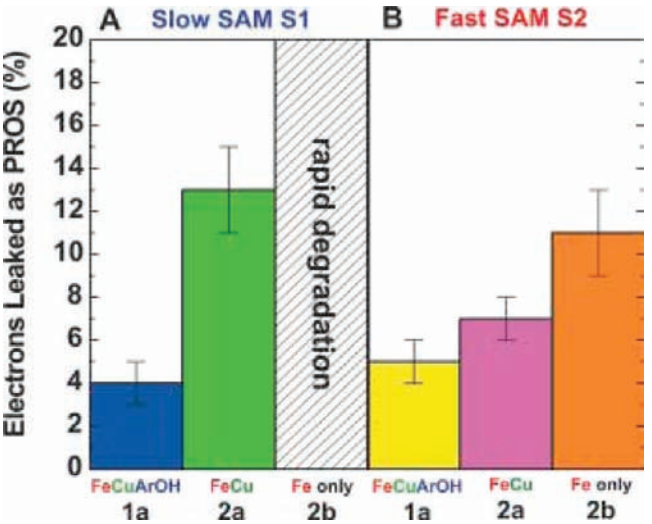

Figure 4. Percentage of PROS formation for slow and fast SAMs on the iron-only, FeCu, and FeCuArOH catalysts.

is not 100% efficient, it will generate PROS (O_2^- or H_2O_2), which can be quantified by comparing the disk and ring currents after calibration of the ring collection efficiency against a known standard.[14] We have also established that the major PROS generated during turnover is superoxide and not peroxide.[24]

The rate of electron transfer between the gold electrode and the iron center in the catalyst is 6 ± 0.1 s^{-1} for the slow SAM and $> 10^4$ s^{-1} (too fast to measure) for the fast SAM. The percentage of electrons supplied by the electrodes that are released as PROS were measured for the catalyst and its analogues (lacking copper and phenol) using both fast and slow SAMs.[22]

Using the fast SAM (Figure 2B), for the iron-only catalyst (lacking copper and phenol), the amount of PROS is ∼11%

(21) Collman, J. P.; Devaraj, N. K.; Eberspacher, T. A.; Chidsey, C. E. D. *Langmuir* **2006**, *22*, 2457–2464.
(22) Collman, J. P.; Devaraj, N. K.; Decreau, R. A.; Yang, Y.; Yan, Y.-L.; Ebina, W.; Eberspacher, T. A.; Chidsey, C. E. D. *Science* **2007**, *315*, 1565–1568.
(23) Bard, A. J.; Faulkner, L. R. *Electrochemical Methods: Fundamentals and Applications*, 2nd ed.; John Wiley & Sons, Inc.: New York, 2001.
(24) Boulatov, R.; Collman, J. P.; Shiryaeva, I. M.; Sunderland, C. J. *J. Am. Chem. Soc.* **2002**, *124*, 11923–11935.

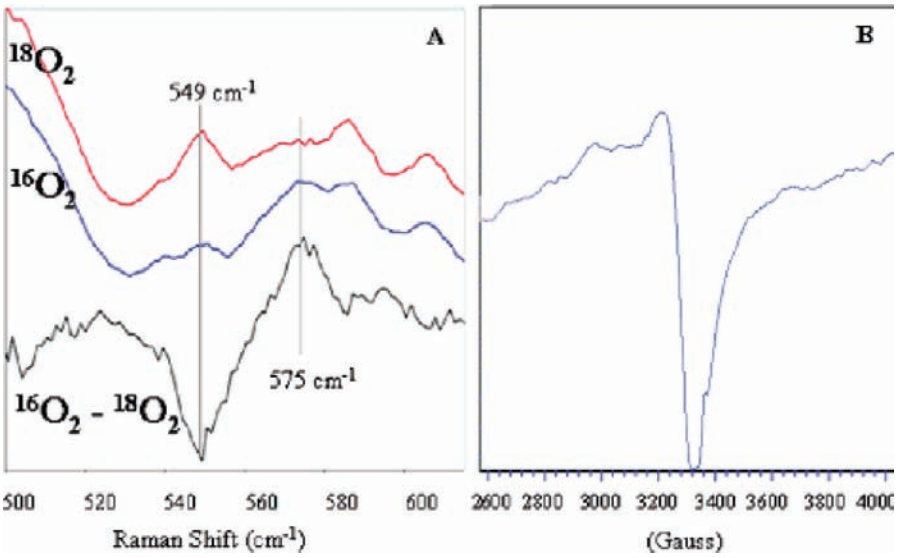

Figure 5. (A) Resonance Raman spectrum of oxygenated FeCuArOH in $^{18}O_2$ and $^{16}O_2$ and their difference spectrum at 77 K in *N*,*N*-dimethylformamide. (B) X-band EPR spectrum obtained upon warming up of the oxy product to −40 °C.

Scheme 4. Plausible Steps for the Generation of PROS

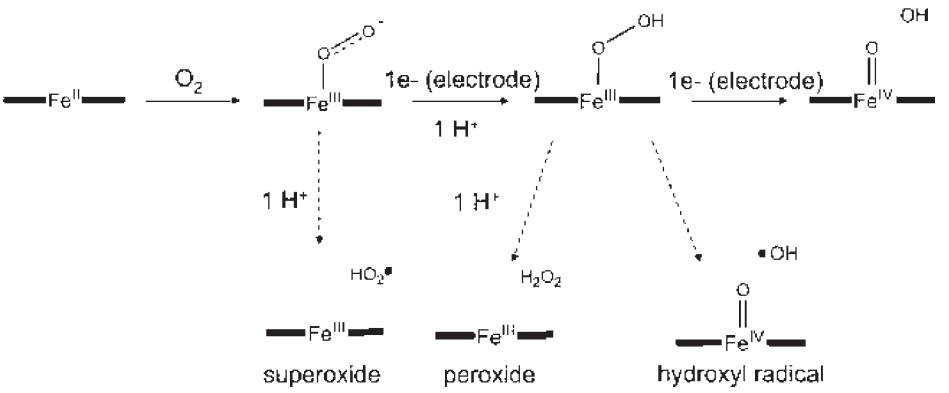

Scheme 5. FeCuArOH Containing All Reducing Electron Equivalents for O_2 Reduction Can Nearly Eliminate PROS Formation

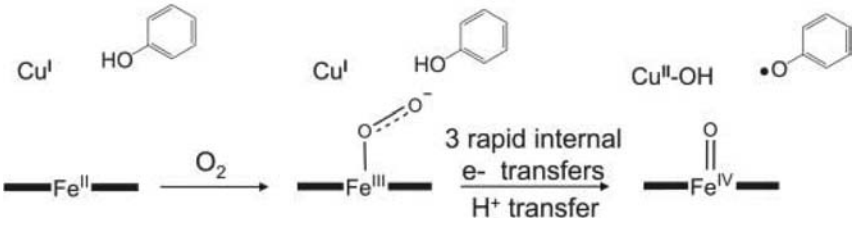

(Figure 4), implying that ∼89% of the electrons are consumed by four-electron reduction of O_2 to H_2O. For the FeCu catalyst (lacking phenol), the amount of PROS generated decreases to ∼7%. However, the amount of PROS generated by the catalyst containing all of the redox active components is reduced to ∼5%, showing phenol has a negligible effect. We propose that, during fast electron transfer from the electrode, phenol does not transfer an additional electron during O_2 reduction. Hence, Tyr^{244} is not essential for supply of the fourth electron when outer-sphere electrons are rapidly transferred.[22]

The slow SAM (Figure 2A) is more biologically relevant because it replicates the slow, physiological electron transfer to the active site. The iron-only complex (lacking copper and phenol) undergoes rapid degradation, possibly because of excessive PROS formation. The FeCu catalyst (lacking phenol) shows ∼13% PROS generation (Figure 4). Because it contains only three electrons (two from Fe^{II} and one from Cu^{I}), this catalyst lacks the fourth electron required for the reduction of O_2 to H_2O. If the electron transfer from the electrode is slow (which is the case for slow SAM), there is an opportunity for the formation and leakage of PROS (Scheme 4). When the complete catalyst is loaded (containing iron, copper, and phenol; Scheme 5), the amount of PROS generated is negligible (∼4%). Thus, phenol acts as the fourth electron source for O_2 reduction, when the electron supply is slow.[22]

The above results clearly demonstrate that the complete catalyst selectively reduces O_2 by four electrons under conditions

Scheme 6. Single-Turnover Reaction Products When FeCuArOH Is Oxygenated: Oxy Formed at −60 °C and Fe^{IV}=O Cupric Phenoxyl Radical Species at −40 °C

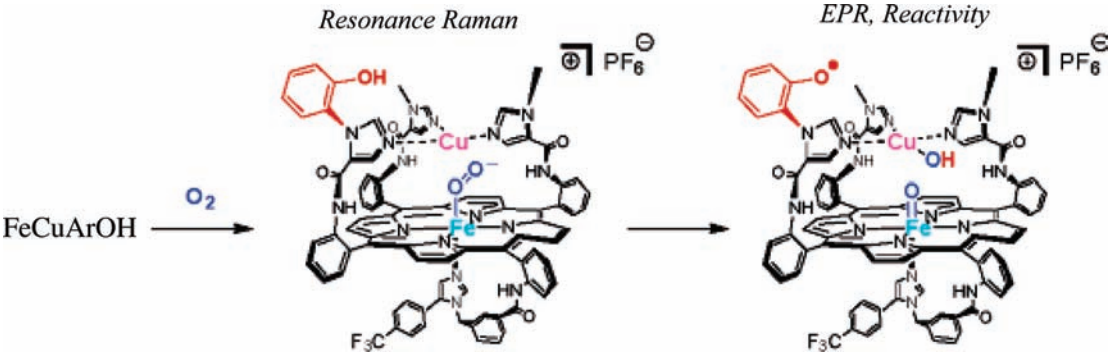

of a slow, rate-limiting electron flux. Although our catalyst is ∼96% selective (∼4% PROS generated), CcO is >99% selective. This imperfect selectivity could arise from differences between the synthetic model and CcO itself. In CcO, O_2 binding occurs only to the fully reduced active site. However, in the case of the synthetic catalyst, O_2 binding may also occur in a mixed-valent form (e.g., Fe^{II}, Cu^{II}), which could lead to leakage of some PROS by hydrolysis of the iron(III) superoxide complex, when electron transfer is too slow. CcO is a membrane-bound protein, but the synthetic catalyst is exposed to H_2O during the electrochemical measurements, which increases hydrolysis, leading to PROS.[22]

4. Single-Turnover O_2 Reduction

The steady-state kinetics of O_2 reduction under slow electron transfer measured electrochemically predicts that the catalyst (having the iron, copper, and phenol residues) stores all four reducing equivalents required for the four-electron reduction of O_2 to H_2O (Scheme 5).

Oxygenation of the catalyst at −60 °C results in the formation of an iron(III) superoxide species.[25,26] This species is electron paramagnetic resonance (EPR) silent and has a Fe−O stretching frequency at 575 cm^{-1}, which shifts to 549 cm^{-1} upon ^{18}O substitution, characteristic of the formation of a heme superoxide species (resonance Raman data; Figure 5A).[27]

Warming the reaction from −60 to −40 °C results in the disappearance of the 575 cm^{-1} peak in the resonance Raman spectrum. The EPR spectrum of the resulting species shows that the copper has been oxidized (Figure 5). We propose that O−O bond cleavage occurs, resulting in the formation of a species having an oxo-Fe^{IV} and a phenoxyl radical, similar to a P_M intermediate[1] (Scheme 6). The oxoferryl nature of this intermediate was confirmed by an oxygen-atom-transfer reaction with triphenylphosphene, forming triphenylphosphene oxide.[27]

The single-turnover study indicates that the phenol acts as a source of protons and electrons for O−O bond cleavage. Generation of a P_M-type (oxo-Fe^{IV}, Cu^{II}, and phenoxyl radical) species demonstrates that the fully reduced catalyst contains all of the electrons required for the four-electron reduction of O_2.

Scheme 7. Plausible Mechanism of O_2 Reduction by Cytc in the Presence of the FeCuPhOH Catalyst

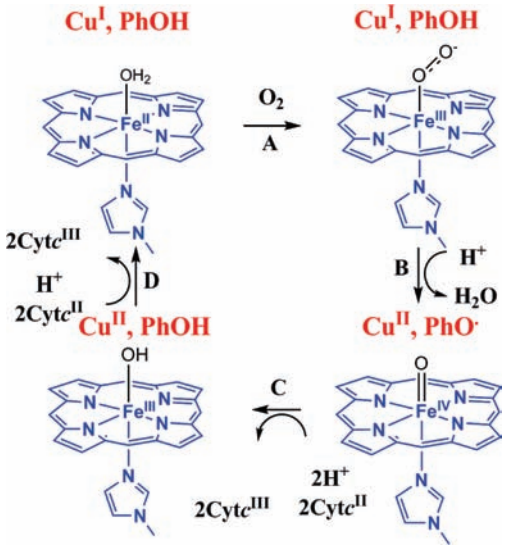

5. Reduction of O_2 by Cytc Using the CcO Model

Cytc is a small electron-transfer protein that is the source of electrons for CcO.[1] In the previous section, it was shown that our functional model catalyzes the selective four-electron reduction of O_2 at physiological pH, using an electrode as the source of electrons generating negligible PROS during catalytic turnover. Our next goal was to selectively catalyze the four-electron reduction of O_2 using the biological one-electron reductant Cytc with this functional CcO model.

Catalytic O_2 reduction using reduced Cytc was studied, using our functional CcO model, under various conditions to gain insight into the mechanism. The O_2 concentration of the solution was measured before and after catalytic turnover and showed that 3.9 ± 0.1 equiv of reduced Cytc is oxidized per molecule of O_2 consumed, indicating that this four-electron oxidation is stoichiometric within experimental error.[28]

A proposed mechanism is presented in Scheme 7. In the first step, O_2 binds to the reduced catalyst, forming an $Fe^{III}-O_2^{\bullet-}$ (superoxide) species (step A). The catalyst contains four electrons, two from Fe^{II}, one from Cu^{I}, and one from phenol, thus forming a species analogous to the P_M intermediate in CcO, comprising of an oxo-Fe^{IV}, an oxidized

(25) Collman, J. P.; Decreau, R. A.; Sunderland, C. J. *Chem. Commun.* **2006**, 3894–3896.
(26) Tsubaki, M.; Nagai, K.; Kitagawa, T. *Biochemistry* (*Moscow*) **1980**, *19*, 379–385.
(27) Collman, J. P.; Decreau, R. A.; Yan, Y.; Yoon, J.; Solomon, E. I. *J. Am. Chem. Soc.* **2007**, *129*, 5794–5795.
(28) Collman, J. P.; Ghosh, S.; Dey, A.; Decreau, R. A.; Yang, Y. *J. Am. Chem. Soc.* **2009**, *131*, 5034–5035.

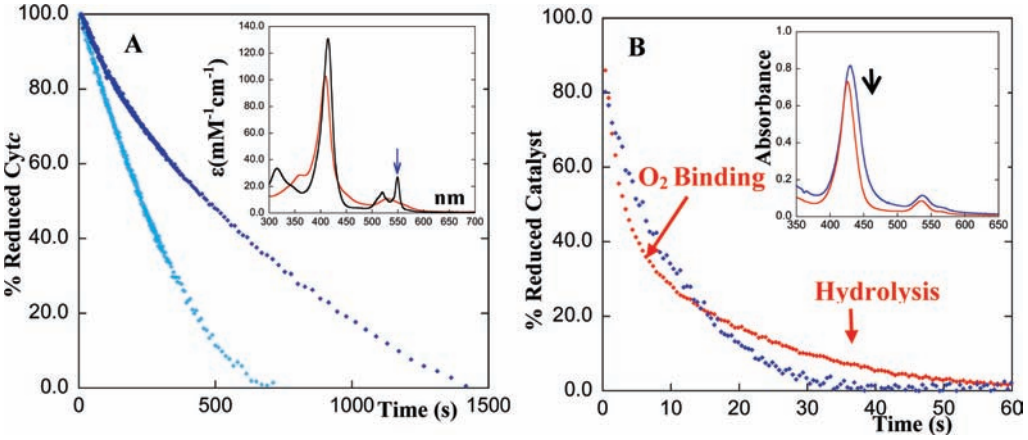

Figure 6. Kinetic traces showing a decrease of (A) reduced Cytc (following the 550 nm band intensity, blue arrow) in the presence of 2% FeCuArOH in aerated (dark blue) and O_2-saturated (light blue) 1:1 aqueous buffer/acetonitrile solvents at pH 7 and 25 °C [inset: absorption spectra of reduced (black) and oxidized (red) Cytc] and (B) reduced catalyst (following the 434 nm absorption intensity, black arrow) in the presence of O_2: iron-only complex (red) and FeCuArOH catalyst (blue) [inset: absorption spectra of the reduced iron-only (red) and FeCuArOH (blue) complexes].

Cu^{II}, and a phenoxyl radical (step B).[27] This P_M intermediate is subsequently reduced by 4 equiv of Cytc to regenerate the fully reduced active catalyst (steps C and D). The possible rate-determining steps (rds) are either (1) O_2 binding, (2) O−O bond cleavage, or (3) electron transfer between Cytc and the oxidized catalyst.

When an O_2-saturated solution is used instead of an air-saturated solution, the turnover rate increases by more than 2-fold (Figure 6A), implying that O_2 binding may be involved in the rds. Upon increasing the concentration of Cytc, while keeping a constant catalyst concentration, the rate of O_2 reduction remains unperturbed. This implies that electron transfer from Cytc is fast and is not the rds. There is also a modest inverse isotope effect of 0.82 for the O_2 reduction kinetics.

The rates of O_2 binding and electron transfer from reduced Cytc to the oxidized catalyst have been determined by following the single-turnover kinetics with the FeCuArOH and iron-only catalysts. The iron-only complex lacks the necessary electron equivalents to undergo O−O bond cleavage and hence acts as a control for the reaction. The reaction of reduced Fe^{II} with O_2 was followed by monitoring of the characteristic Fe^{II} absorption at 434 nm (Figure 6B, red). The rate of O_2 binding, resulting in the formation of iron(III) superoxide species, was found to be 0.5 s^{-1}, followed by its slow hydrolysis (0.05 s^{-1}). Similarly, following the Fe^{II} absorption intensity of the FeCuArOH catalyst (Figure 6B, blue) shows a monophasic kinetic behavior with a rate constant of 0.1 s^{-1}, resulting in the formation of a $Fe^{III}Cu^{II}$ species. Because the FeCuArOH catalyst reduces O_2 stoichiometrically (vide supra) and the amount of hydrolysis side reaction is negligible (PROS < 4%), the monophasic kinetics of the O_2 reaction (i.e., no further intermediates observed) implies that O−O bond cleavage (step B, Scheme 1) and decay of the high-valent intermediate (step C, Scheme 1) must be much greater than 0.1 s^{-1}. This implies that O_2 binding is the rds.

Note that the rate of O_2 binding to the fully reduced FeCuArOH catalyst is slower than that of the iron-only complex, possibly because of greater steric hindrance in the former due to the phenol substituent, making O_2 binding even slower. The rate of O_2 binding to our catalyst is much slower than those reported for the actual CcO enzyme and other heme proteins and model complexes.[1] This slow O_2 binding is due to an axial water ligand in the distal pocket, which further hydrogen bonds to other H_2O molecules, making the ferrous center low spin, in contrast to the five-coordinate high-spin ferrous active site found in CcO.[29] The observed inverse kinetic isotope effect is consistent with the displacement of H_2O by O_2 in the rds.

The rates of electron transfer between reduced Cytc and oxidized $Fe^{III}Cu^{II}$ArOH catalysts or the Fe^{III}-only complex (step D, Scheme 1), under anaerobic conditions, were estimated to be ~1.2 s^{-1} during catalytic turnover. The rate of O_2 binding (0.1 s^{-1}) is at least 10 times slower than the rate of electron transfer from reduced Cytc to the $Fe^{III}Cu^{II}$ArOH catalyst. The rate of reduction of P_M (Scheme 7, step C) should be even greater than the rate of reduction of $Fe^{III}Cu^{II}$ because the former has a much larger driving force. Thus, we conclude that the rate of O_2 binding is the rds during catalytic O_2 reduction by Cytc. The rates of O−O bond cleavage and electron-transfer steps are faster.[28]

6. Modeling the Protective Role of NO in CcO

NO, generated in the mitochondria by the enzyme NO synthase, plays a key role in controlling respiration.[30,31] It is an acute competitive inhibitor of CcO because it binds the active site rapidly ($k_{on} \sim 10^8$ M^{-1} s^{-1}) and tightly ($K_D < 10^{-9}$ M).[32,33] However, inhibition by NO is reversible. We explored the reaction of NO with our functional model to understand the mechanism behind this reversible inhibition and discovered how NO might protect CcO from other potent inhibitors.[34]

When the iron-only (lacking copper and phenol) and FeCu (lacking phenol) catalysts were exposed to 1 equiv of NO, the Soret and Q bands were significantly perturbed (blue to

(29) Collman, J. P.; Decréau, R. A.; Dey, A.; Yang, Y. *Proc. Natl. Acad. Sci. U.S.A.* **2009**, *106*, 4101–4105.
(30) Ghafourifar, P.; Richter, C. *FEBS Lett.* **1997**, *418*, 291–296.
(31) Giulivi, C.; Poderoso, J. J.; Boveris, A. *J. Biol. Chem.* **1998**, *273*, 11038–11043.
(32) Ford, P. C.; Lorkovic, I. M. *Chem. Rev.* **2002**, *102*, 993–1017.
(33) Brunori, M.; Forte, E.; Arese, M.; Mastronicola, D.; Giuffre, A.; Sarti, P. *Biochim. Biophys. Acta* **2006**, *1757*, 1144–1154.
(34) Collman, J. P.; Dey, A.; Decreau, R. A.; Yang, Y.; Hosseini, A.; Solomon, E. I.; Eberspacher, T. A. *Proc. Natl. Acad. Sci. U.S.A.* **2008**, *105*, 9892–9896.

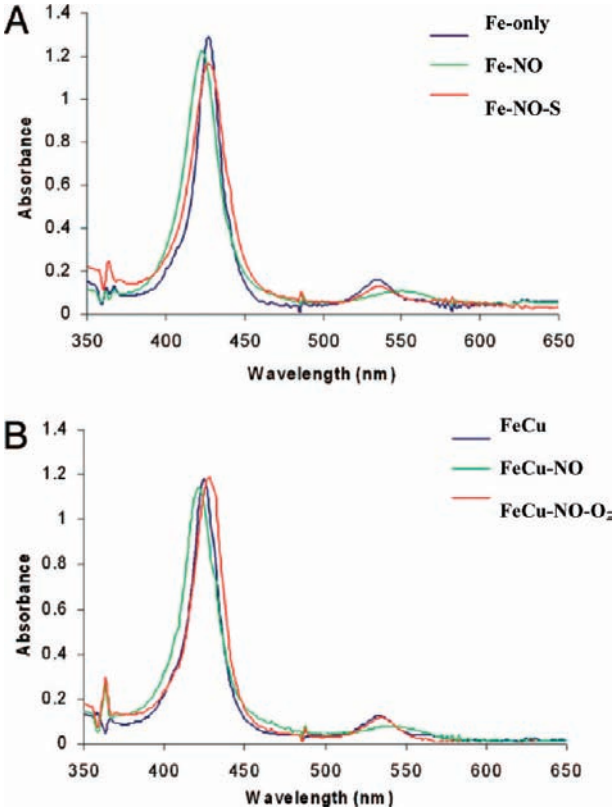

Figure 7. Absorption spectra of the NO derivatives and their reaction with O_2 and superoxide for iron-only (A) and FeCu (B) complexes.

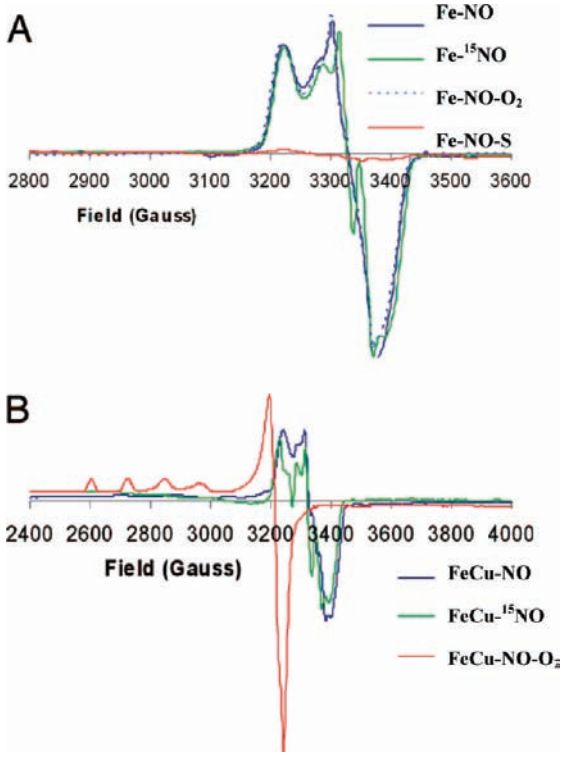

Figure 8. EPR spectra of the NO derivatives and their reaction with O_2 and superoxide for iron-only (A) and FeCu (B) complexes.

green; Figure 7A,B), implying the binding of NO to the active site. The EPR spectra of these NO complexes (Figure 8A,B) are characteristic of low-spin, six-coordinate $S = {}^1/_2$ iron nitrosyl species, with $g_z = 2.078$, $g_y = 2.015$, and $g_x = 1.97$, having multiple ^{14}N superhyperfine in the A_y region, which is perturbed by isotopically enriched ^{15}NO.

When the iron-only nitrosyl (Fe−NO) species is exposed to excess O_2, the UV−vis and EPR data are unperturbed (no reaction occurs). When the iron-only nitrosyl (Fe−NO) species is exposed to 1 equiv of superoxide (Fe−NO−S), the UV−vis spectrum changes, resulting in a ferrous species (similar to the starting compound), and there is a loss of the ferrous nitrosyl signal in the EPR spectrum (Figures 7A and 8A). Moreover, when the FeCu nitrosyl species (FeCu−NO) is exposed to O_2 (FeCu−NO−O_2), the UV−vis data change, yielding a spectrum similar to the starting iron-only ferrous species. The EPR spectrum of the oxygenated product shows a loss of the ferrous nitrosyl signal, with the formation of another $S = {}^1/_2$ signal, which is typical of a type 2 Cu^{II} species (Figures 7B and 8B). The lack of appearance of any EPR signals for both Fe−NO−S and FeCu−NO−O_2 even at 4 K suggests the absence of any high-spin ferric species. The above observations are summarized in Scheme 8.

The ferrous nitrosyl species (Fe−NO) is inert toward O_2, but in the presence of superoxide, it forms a ferrous species. We propose that when the distal Cu^I is present, the nitrosyl species reacts with O_2, generating superoxide in situ. This superoxide then reacts with the ferrous nitrosyl to generate a ferrous species, similar to the iron-only complex. This intramolecular reaction probably proceeds via a peroxynitrite intermediate formed by reaction between superoxide and the NO complex. The putative peroxynitrite should readily isomerize into nitrate in organic solvents.[35] This reaction (destabilization of ferrous nitrosyl species) provides a possible mechanism for the recovery of CcO from inhibition by NO, requiring both the distal copper and oxygen.

Carbon monoxide (CO) and cyanide (CN^-) are well-known potent inhibitors of CcO and either are present in the human body or are introduced into the body by our diet. When the iron-only complex is exposed to CO, it generates a UV−vis spectrum with a sharp Soret band, characteristic of a ferrous carbonyl species (Fe−CO; Figure 9A). Similarly, when the iron-only complex is exposed to CN^-, the UV−vis spectrum is modified, indicative of the formation of a ferrous cyanide complex (Fe−CN; Figure 9A). We observed that when equimolar amounts of NO are introduced to Fe−CO and Fe−CN, the CO and CN^- ligands are replaced. This was further supported by EPR experiments (Figure 9B). The Fe^{II}−CN complex is diamagnetic and EPR-silent. The EPR spectrum of the Fe−CN complex treated with NO is identical with the Fe−NO complex having a characteristic $S = {}^1/_2$ ferrous nitrosyl signal, implying replacement of CN^- by NO.

Amyl nitrite (AmN) is used medically for the treatment of CN^- exposure. When AmN is added to the FeCu cyanide species (FeCu−CN), it generates an EPR spectrum characteristic of the presence of $S = {}^1/_2$ Cu^{II} species and $S = {}^1/_2$ ferrous nitrosyl species (total spin integration accounts for the presence of two paramagnetic centers; Figure 9B). On the basis of these observations, we propose a mechanism for recovery from CN^- poisoning shown in Scheme 9. We believe that AmN is reduced by Cu^I into amyl alkoxide and NO, generating Cu^{II} (an oxidative addition reaction). NO generated from AmN replaces the cyanide bound to the ferrous site, forming an iron nitrosyl species.

(35) Koppenol, W. H.; Kissner, R.; Beckman, J. S. *Methods Enzymol.* **1996**, *269*, 296–302.

Scheme 8. Proposed Reaction Mechanism of Removal of NO from CcO Using the Iron-Only and FeCu Catalysts

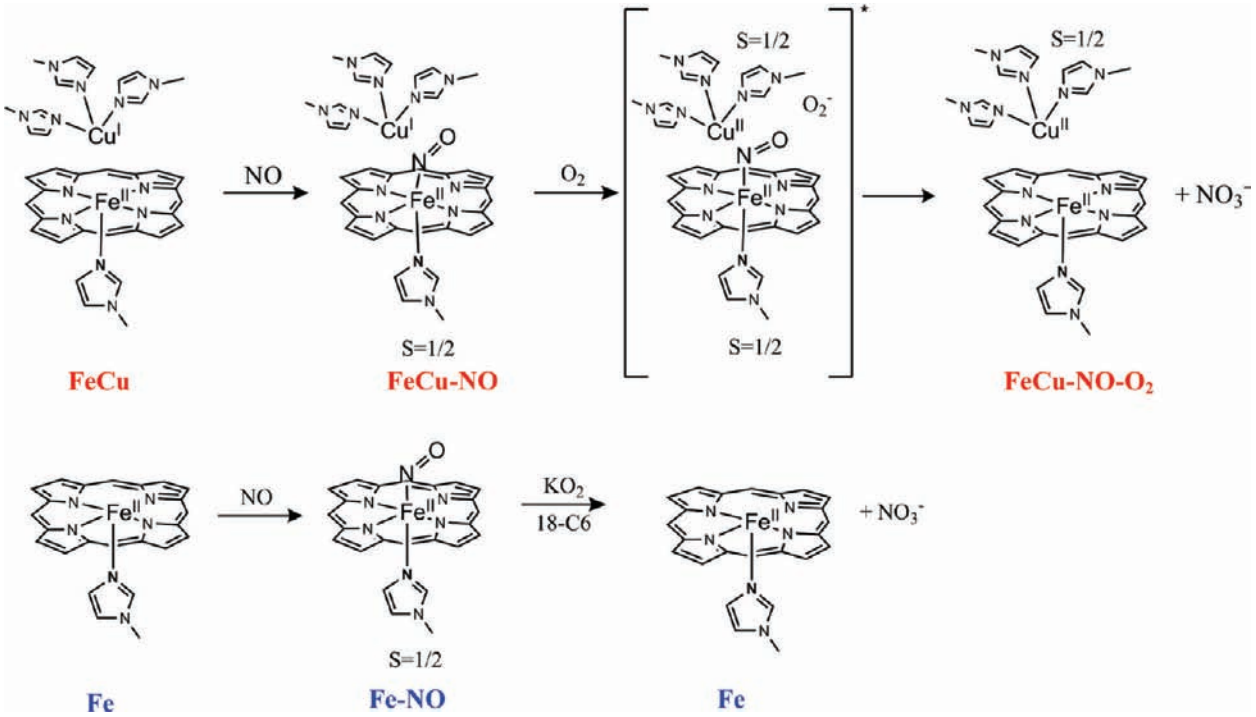

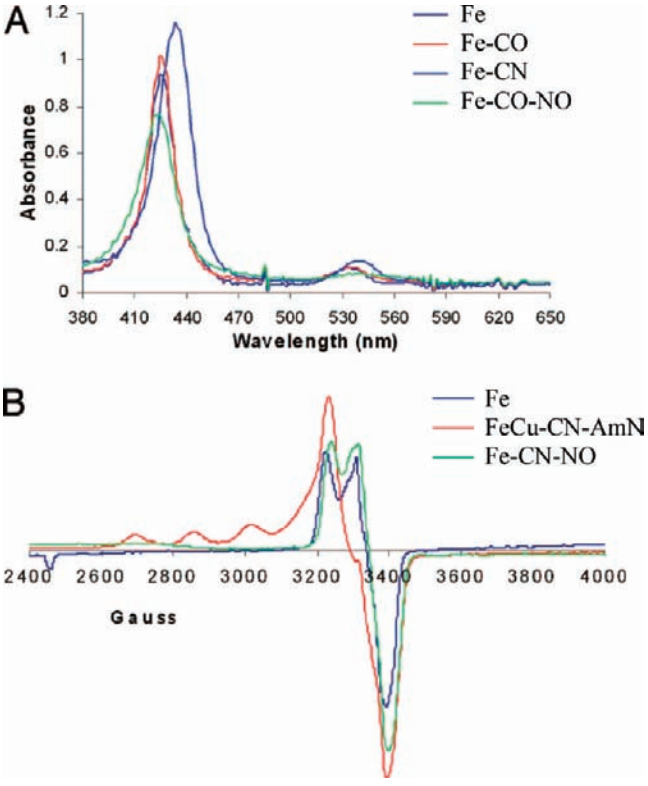

Figure 9. Absorption (A) and EPR (B) spectra of CO and CN derivatives of iron and FeCu and their reactions with NO and AmN, respectively.

The above results clearly demonstrate how the active site of CcO could be revived from inhibition by NO, which is generated close to the CcO active site by NO synthase. Also, the greater affinity of NO for the reduced active site endows it with the intriguing capability of protecting CcO from inhibition by other potent inhibitors like CO and CN^-. Our predictions for the protective role of CcO by NO were more recently tested in the real enzyme system and found to hold true.[36]

7. Elucidating the Role of H_2S Inhibition of CcO

H_2S is produced in humans and other mammals by two enzymes, cystathione γ-lyase and cystathione β-synthase, which act on a simple amino acid, L-cysteine.[37,38] Long-term exposure to H_2S is reported to produce cytotoxic effects such as cerebral stroke, inflammatory diseases, mental retardation, and cell death.[39,40] However, in lower, micromolar concentrations, H_2S induces various cytoprotective effects. It stimulates ATP-sensitive potassium channels, causing inhibition of insulin secretions in smooth-muscle cells, neurons, cardiomyocytes, and pancreatic β cells.[37,38,41] H_2S has been recently found to induce hypothermia in mice when exposed to a moderate (~80 ppm) dosage, resulting in a dramatic decrease in the core body temperature to a level as low as 15 °C, and their metabolic rate is decreased by nearly 90%.[42−44] This phenomenon appears similar to hibernation and aestivation, which have been observed in other mammals, reptiles, and amphibians.[43,45] The stimulation of

(36) Pearce, L. L.; Elisenda, L. M.; Martinez-Bosch, S.; Peterson, J. *Chem. Res. Toxicol.* **2008**, *21*, 2073–2081.
(37) Szabo, C. *Nat. Rev. Drug Discovery* **2007**, *6*, 917–935.
(38) Wang, R. *FASEB J.* **2002**, *16*, 1792–1798.
(39) Dorman, D. C.; Moulin, F. J.-M.; McManus, B. E.; Mahle, K. C.; James, R. A.; Struve, M. F. *Toxicol. Sci.* **2002**, *65*, 18–25.
(40) Khan, A. A.; Schuler, M. M.; Prior, M. G.; Yong, S.; Coppock, R. W.; Florence, L. Z.; Lillie, L. E. *Toxicol. Appl. Pharmacol.* **1990**, *103*, 482–490.
(41) Lowicka, E.; Beltowski, J. *Pharmacol. Rep.* **2007**, *59*, 4–24.
(42) Blackstone, E.; Morrison, M.; Roth, M. B. *Science* (*Washington, DC*) **2005**, *308*, 518–518.
(43) Lee, C. C. *Annu. Rev. Med.* **2008**, *59*, 177–186.
(44) Volpato, G. P.; Searles, R.; Yu, B.; Scherrer-Crosbie, M.; Bloch, K. D.; Ichinose, F.; Zapol, W. M. *Anesthesiology* **2008**, *108*, 659–668.
(45) Heldmaier, G.; Ortmann, S.; Elvert, R. *Respir. Physiol. Neurobiol.* **2004**, *141*, 317–329.

Scheme 9. Proposed Mechanism for the Protection of CcO from Cyanide, Using Amyl Nitrite

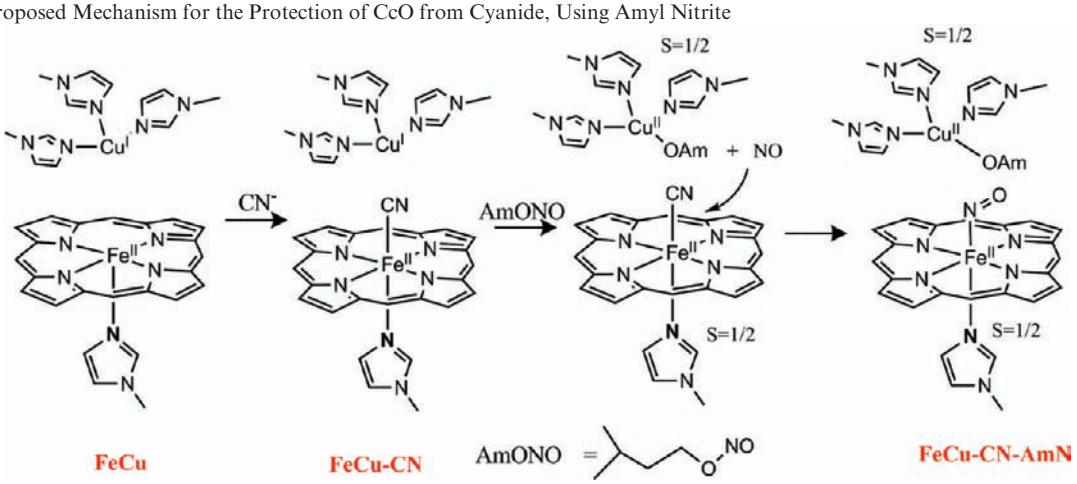

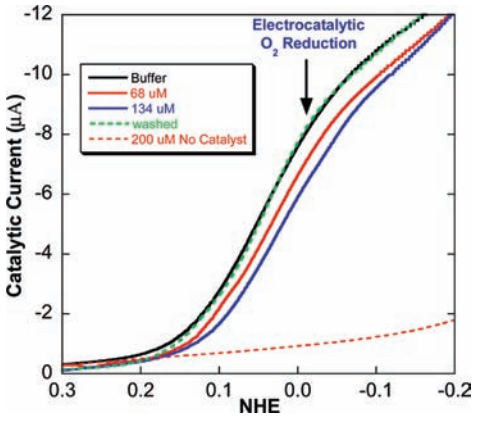

Figure 10. Linear-sweep voltammogram of the FeCuArOH catalyst modified electrode showing a catalytic O_2 reduction current in the absence of NaSH (black), in the presence of 68 μM NaSH (red) and 134 μM NaSH (blue), after removal of NaSH (dotted green), and in 200 μM NaSH in the absence of any catalyst (dotted red).

hypothermia has many possible medicinal applications in ischemia, pyrexia, reperfusion conditions, preservation of transplant organ, traumas, during surgery, etc.[37,42,46]

H_2S has been proposed to be a reversible competitive inhibitor of CcO, hence slowing respiration. However, at lower concentrations, H_2S has been claimed to be a noncompetitive inhibitor of CcO.[47,48] We have used our functional CcO model to explore the different effects that H_2S might have on mitochondria at different concentrations.[49]

The electrocatalytic current representing the catalytic O_2 reduction of the CcO model on a linear-sweep voltammogram on modified electrodes decreases when H_2S ($pK_a = 7$) is introduced from an NaSH buffer solution (Figure 10). The catalytic O_2 reduction at 0 mV vs NHE is almost fully recovered (95−100%) when the NaSH buffer is replaced by an air-saturated buffer, thus removing H_2S. These electrocatalytic experiments with our functional model show how H_2S could reversibly inhibit CcO and slow respiration.

When NaSH in a pH 7 buffer solution is added anaerobically to the reduced $Fe^{II}Cu^{I}$ArOH catalyst, the Soret band of the porphyrin becomes slightly red-shifted with decreased intensity and the Q-band intensity is slightly increased (Figure 11, black to red), indicating that H_2S binds to the reduced active site. The sequential addition of H_2S to the $Fe^{II}Cu^{I}$ analogue was monitored by following its UV−vis spectra to determine the binding affinity of H_2S to the reduced metals. The data indicate that two molecules of H_2S bind the reduced catalyst with approximate binding constants of 0.8 and 0.1, implying a weak binding. The H_2S-bound complexes have been further characterized by ^{1}H NMR, IR, and mass spectroscopies.[49]

The weak binding of H_2S has been probed by ligand replacement experiments. When the H_2S-bound $Fe^{II}Cu^{I}$ArOH complex is exposed to CO (Figure 11A, blue), it generates a spectrum characteristic of the formation of a Fe^{II}−CO complex. This indicates that H_2S can be replaced by stronger ligands like CO. In order to determine whether O_2, the physiological substrate of CcO, could replace H_2S bound to the reduced catalyst, the Fe^{II}ArOH complex was used. This complex lacks all of the necessary reducing equivalents (one additional reducing equivalent from Cu) for O−O bond cleavage and therefore would not reduce O_2. When O_2 is added to the H_2S-bound Fe^{II}ArOH complex (Figure 11B, red), it generates a spectrum characteristic of an $Fe^{III}-O_2^-$ complex (Figure 11, green), implying that the bound H_2S is readily replaced by O_2. These results demonstrate that, although H_2S binds to the reduced $Fe^{II}Cu^{I}$ArOH site, it is not a strong ligand and can be replaced by either CO or O_2.

H_2S is known to be a two-electron-reducing agent and has been reported to reduce metal centers in CcO.[50,51] When 1 equiv of a NaSH solution (in a pH 7 buffer) is added to the oxidized CcO model, quantitative reductions of both the Fe^{III} heme and distal Cu^{II} centers are observed, generating the spectrum of the $Fe^{II}Cu^{I}$ArOH catalyst (Figure 12A, black). This reaction was also followed using EPR spectroscopy. The EPR spectrum of the $Fe^{III}Cu^{II}$ complex [in frozen tetrahydrofuran (THF); Figure 12B, red] shows a low-spin Fe^{III} signal overlapping with the Cu^{II} signal between 2200 and 3800 G. The addition of 1 equiv of tetra-*n*-butylammonium

(46) Blackstone, E.; Roth, M. B. *Shock* **2007**, *27*, 370–372.
(47) Cooper, C. E.; Brown, G. C. *J. Bioenerg. Biomembr.* **2008**, *40*, 533–539.
(48) Petersen, L. C. *Biochim. Biophys. Acta* **1977**, *460*, 299–307.
(49) Collman, J. P.; Ghosh, S.; Dey, A.; Decreau, R. A. *Proc. Natl. Acad. Sci. U.S.A.* **2009**, *106*, 22090–22095.
(50) Hill, B. C.; Woon, T.; Nicholls, P.; Peterson, J.; Greenwood, C.; Thomson, A. J. *Biochem. J.* **1984**, *224*, 591–600.
(51) Nicholls, P.; Kim, J. K. *Can. J. Biochem.* **1982**, *60*, 613–623.

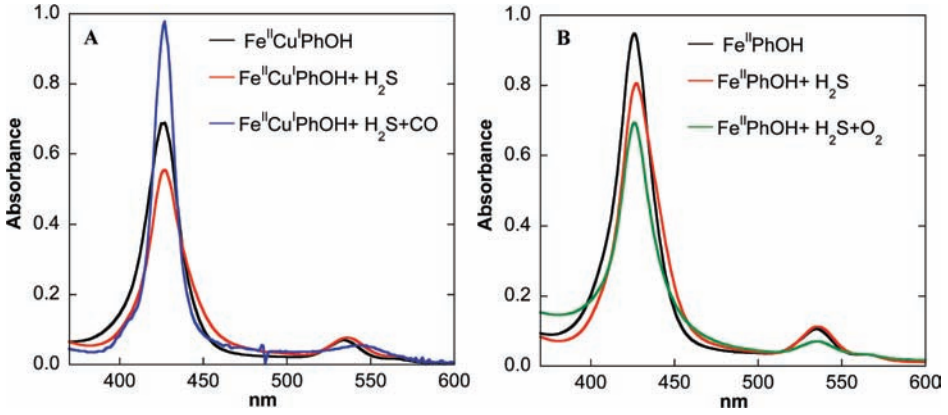

Figure 11. UV−vis spectra of (A) reduced 5 μM $Fe^{II}Cu^{I}$ArOH (black), reduced $Fe^{II}Cu^{I}$ArOH + 0.5 mM NaSH solution (red), and reduced Fe^{II}ArOH + 0.5 mM NaSH solution + excess CO gas (blue) and (B) reduced 8 μM Fe^{II}ArOH (black), reduced Fe^{II}ArOH + 80 μM NaSH solution (red), and reduced Fe^{II}ArOH + 80 μM NaSH solution + excess O_2 gas (green).

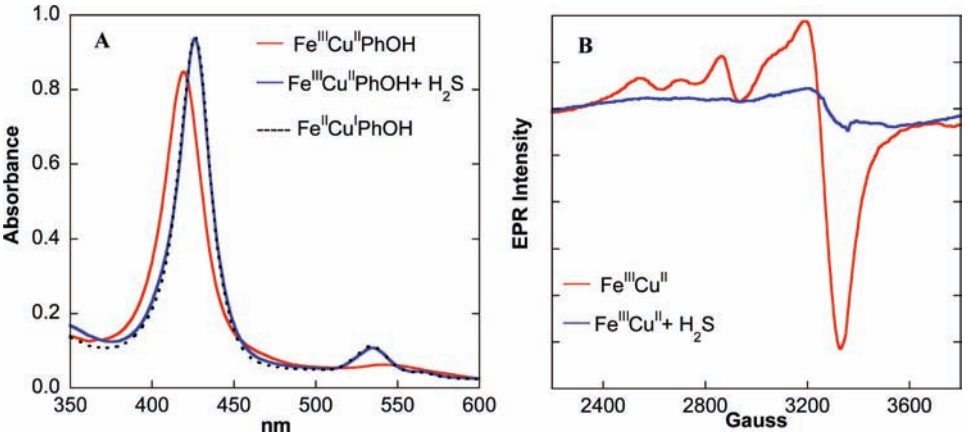

Figure 12. (A) UV−vis spectra (in a 50:50 volume ratio of a pH 7 aqueous buffer and acetonitrile) of 10 μM oxidized $Fe^{III}Cu^{II}$ArOH (red) and oxidized $Fe^{III}Cu^{II}$ArOH + 70 μM NaSH solution (blue) overlaid with a reduced $Fe^{II}Cu^{I}$ArOH spectrum (dotted black). (B) EPR spectra of 1 mM oxidized $Fe^{III}Cu^{II}$ (red) in THF and oxidized $Fe^{III}Cu^{II}$ + 1 mM tetra-*n*-butylammonium hydrosulfide solution (blue) at 77 K.

hydrosulfide results in a loss of this signal. We have further demonstrated that H_2S also quantitatively reduces oxidized Cytc, the electron source for CcO. These results show that H_2S can completely reduce both the oxidized CcO complex and Cytc, even at very low H_2S concentrations.

Scheme 10 illustrates the different interactions between H_2S and CcO at different concentrations based on studies with our model CcO complexes. At high concentrations, H_2S should competitively bind to the reduced active site of CcO, competing with its substrate O_2 binding to the reduced active site.[49] However, this inhibition should be reversible because O_2 can readily replace H_2S, as demonstrated by the ligand binding studies. This hypothesis is further supported by the electrochemical experiments showing that, as H_2S gets flushed from the system, the catalytic current representing O_2 reduction is almost completely restored. These results are similar to the effect that H_2S is reported to have on respiration in mammals, i.e., reversible inhibition at higher concentrations. H_2S can also act as a potent reductant, quantitatively reducing the active site of CcO even at low concentrations. Thus, H_2S could provide reducing equivalents to the active site of CcO during O_2 reduction. Moreover, H_2S can also reduce Cytc, which normally derives its reducing equivalents from food metabolism. Consequently, H_2S might serve as a source of electrons during periods of hibernation when food supplies are low.

Scheme 10. Schematic Representation of the Possible Roles of H_2S Affecting CcO Activity[a]

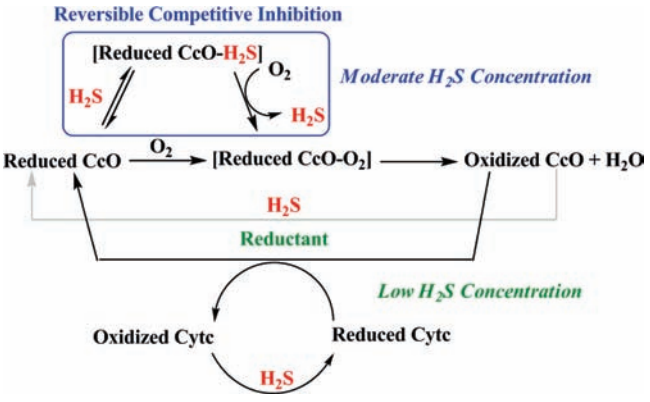

[a] The blue box indicates that, at moderate concentrations, H_2S binds to the reduced CcO active site but can be subsequently replaced by O_2. At lower concentrations, H_2S can reduce CcO's active site and/or Cytc during catalytic O_2 reduction.

8. Summary

This research began by the development of a model complex that is structurally similar to the active site in CcO. In a single-turnover experiment, this complex reduces

O_2 by four electrons, generating an intermediate similar to P_M in the enzyme. This synthetic model was then shown to be a functional mimic of CcO. Methods were developed, using SAMs and click chemistry to create a biomimetic model for the selective four-electron electrocatalytic reduction of O_2 under physiological conditions of slow, rate-limiting electron transfer. Finally, it has been demonstrated that this functional CcO model can be used to understand real biological phenomena: interactions of NO with CcO and the chemistry behind the induction of hibernation. Thus, this research makes a rare connection between synthetic models and biological phenomena.

Acknowledgment. Various aspects of this research have been generously supported by the National Institutes of Health and the National Science Foundation. We thank all past and present students, postdocs, and collaborators for their contributions to the research described.